HARMONIC DETECTION NEURAL APPROACH FOR SINGLE-PHASE ACTIVE POWER FILTER

Claudionor F. Nascimento[*], Azauri A. Oliveira Jr.[*], Alessandro Goedtel[‡], Ivan N. Silva[*]
[*]University of Sao Paulo, Sao Carlos SP
[‡]Federal University of Technology - Parana, Cornelio Procopio PR
{cfnascim, azaurijr, insilva}@sel.eesc.usp.br, agoedtel@utfpr.edu.br

Abstract **– In this paper an alternative method is presented based on artificial neural networks for the determination of the current harmonic components of nonlinear load in single-phase line, whose amplitudes and angles of phase present uncertainties in steady state response. The nonlinear load is composed by an AC controller with variable resistive load. The effectiveness of the proposed method and its application in simulated single-phase active power filters with selective harmonic compensation are verified. Simulation and experimental results are presented to validate the proposed approach**

Keywords **- Harmonic Determination, Single-Phase Active Power Filter, Artificial Neural Network.**

I. INTRODUCTION

The growing use of loads producing harmonic currents causes the proportional increase of disturbances originated by the harmonic distortion in electric systems. The harmonic pollution due to the single-phase loads individually has small power, but when used in large numbers in electric systems can cause significant harmonic distortion problems. This pollution is not restricted only in industry, but also it is present in home appliances and commerce. Besides, the harmonic current flowing through the system causes undesirable effects [1,2,3].

The problems related to the harmonic distortion can be solved by using filters with the objective to cancel the system harmonic components. There are two general classes of filters for the harmonic distortion correction. The first class is based on the use of conventional passive filters, but this one can present resonance problems as much with the line feed impedance as to the other system loads. Besides, these filters are not appropriate to be used in system susceptible to loads that present variable harmonic contents. The second class consists on active power filters. The active filters have showed themselves, nowadays, an effective solution in the correction of the harmonic distortion in a versatile way [3-8].

Among the several possible configurations to the accomplishment of the Active Power Filter (APF), the topology denominated Parallel Active Power Filter (PAPF) has been the most broadly used nowadays. Its configuration is made of a principle voltage source inverter connected in parallel with the load (Figure 1). Its work is to inject an appropriate current to the Point of Common Coupling (PCC) of the system, canceling the harmonic components from the drained current of the voltage source [2]. The compensation features of a PAPF are defined mainly for the used strategy to determine the harmonic content of the load current and to generate the reference current of its control system. This reference current determination has been done through two approaches: the first is named time domain approach [2], and the second is frequency domain approach [1,6,7]. In the frequency domain, the most used technique nowadays to the reference current determination is based on the Discrete Fourier Transform (DFT) [6,7,9,10].

An alternative and promising tool to DFT is the use of Intelligent Systems (IS) in the estimation process of the harmonic content of the current signal. Among the several IS technique the most used are the Artificial Neural Network (ANN) ones [11-16]. In some cases the ANN is able to identify the main harmonic components of the Fourier series [11]. There is also the possibility to use one or more ANN architecture joined to the harmonic compensation system, for example, an ADALINE to the harmonic determination and a multilayer perceptron to the active filter controller [13].

The proposal of this work is to present a method based on ANN to determine the six first harmonic components of the load current in a single-phase line, which are used to the reference current determination of the PAPF to the selective compensation. The determination of these harmonic components is made by sampling in a half period cycle of the voltage source. The on-line ANN is used due to the uncertainties of the systems in steady-state, i.e., the circuit operations might change depending on the load operating condition and parameter variation.

The single-phase load used in this paper is composed by an AC controller feeding three incandescent lamps setting of 100 W each, performing a regulator of luminous intensity (dimmer) [1], showed in Figure 1. The current waveforms characteristics of this load can be varying in time. The ANN training is done in an off-line form, through previous knowledge of the harmonic behavior of the load. After this training has been made, the ANN identifies in an on-line way each harmonic component starting from the amplitudes of the current of the load which are sampled and presented at the input of the ANN [1].

This work is organized in five sections. In Section 2 the load features and the studied system aspects are presented. In Section 3, it is reported the involved principles with the neural approach. In Section 4 the simulation results of the active filters are presented. Finally, in Section 5, the paper conclusions are described.

II. HARMONIC CURRENT

The AC controller showed in Figure 1 represents a nonlinear load to the voltage source. This controller is made by a TRIAC *A*, a sinusoidal voltage source $\{v_S(t)\}$, a firing circuit, and a incandescent lamps with a resistive behavior (*R*). The harmonic components amplitudes and phases of this

system vary as with the TRIAC firing angle as with the resistance behavior of the lamps.

The nonlinear load voltage $v_L(t)$, as a function of the firing angle α, can be solved by n-th (n odd) harmonic, i.e.:

$$v_L(t) = \frac{V}{\pi}\left\{\frac{1}{2}[\cos 2\alpha - 1]\cos\omega t + \frac{1}{2}[\sin 2\alpha + 2\pi - 2\alpha]\sin\omega t + \sum_{n=3}^{\infty}\left[\frac{\cos(n+1)\alpha - \cos(n+1)\pi}{n+1} - \frac{\cos(n-1)\alpha - \cos(n-1)\pi}{n-1}\right]\cos n\omega t + \sum_{n=3}^{\infty}\left[\frac{\sin(n+1)\alpha}{n+1} - \frac{\sin(n-1)\alpha}{n-1}\right]\sin n\omega t\right\} \quad (1)$$

where:

V - Voltage source amplitude.

ω - Fundamental angular frequency.

The load current representation $i_L(t)$ can be taken as

$$i_L(t) = \frac{v_L(t)}{R} \quad (2)$$

The lamps resistances vary with the temperature and, consequently, with the RMS (Root Mean Square) voltage, which vary with the TRIAC firing angle (α), according to (3). The RMS voltage value can also be, approximately, calculated by voltage n-th harmonic of output $\{V_n\}$ by (3).

$$V_{RMS} = V\sqrt{\frac{1}{2} - \frac{\alpha}{2\pi} + \frac{\sin 2\alpha}{4\pi}} \cong \sqrt{\sum_{n=1}^{N}\frac{V_n^2}{2}} \quad (3)$$

where N is the number of harmonics. The current n-th harmonic amplitude component $\{I_n\}$ is given by (4). Figure 2 shows the variation of RMS load current $\{I_{RMS}\}$, that can be calculated in relation to α, or approximately by (5).

$$I_n = \frac{V_n}{R} \quad (4)$$

$$I_{RMS} = \frac{V_{RMS}}{R} = \frac{V}{R}\sqrt{\frac{1}{2} - \frac{\alpha}{2\pi} + \frac{\sin 2\alpha}{4\pi}} \cong \sqrt{\sum_{n=1}^{N}\frac{I_n^2}{2}} \quad (5)$$

The Total Harmonic Distortion (THD) [17] is given by (6). Equation (7) presents the harmonic distortion influence in the RMS load current.

$$THD = \frac{\sqrt{\sum_{n=2}^{\infty} I_n^2}}{I_1} \quad (6)$$

$$I_{RMS} = \frac{I_1}{\sqrt{2}}\sqrt{1 + THD^2} \quad (7)$$

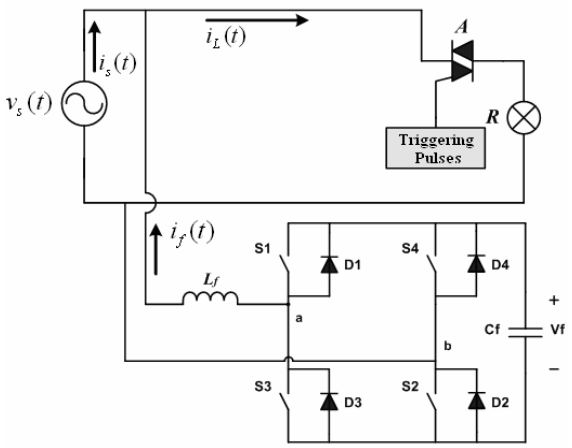

Fig. 1. System with a PAPF and an AC controller.

Figure 2 shows the current THD variation as a function of the firing angle of the TRIAC A. The six first load current harmonic components variation of the system in function to the AC controller firing angle is presented in Figure 3. It is observable that above 150º all the amplitudes get close to the fundamental component value increasing the distortion (above 180%, Figure 2), but with smaller impact in the system due to their small amplitudes [1].

III. HARMONIC DETEMINATION

The network architecture used in this work has 42 inputs, which they receive from the AC controller sampled current in a half cycle of line voltage with sampling rate of 5.04 kHz, as shown in Figure 4. The first layer (hidden) has five neurons, and the second layer has one neuron (output) (Figure 5). The activation function of each neuron of the first layer is the hyperbolic tangent while activate function of the second layer neuron is linear. This architecture repeats for each component (1st, 3rd, 5th, 7th, 9th, and 11th).

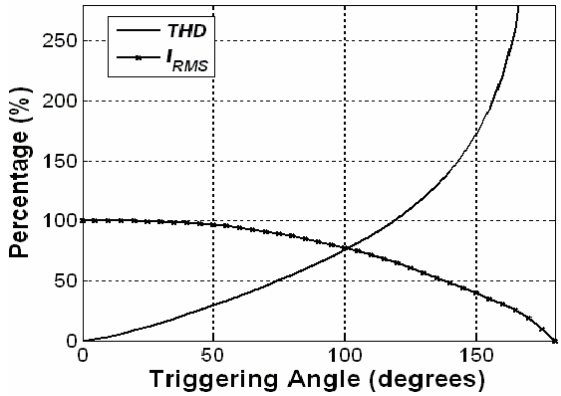

Fig. 2. RMS current and THD in function of firing angle.

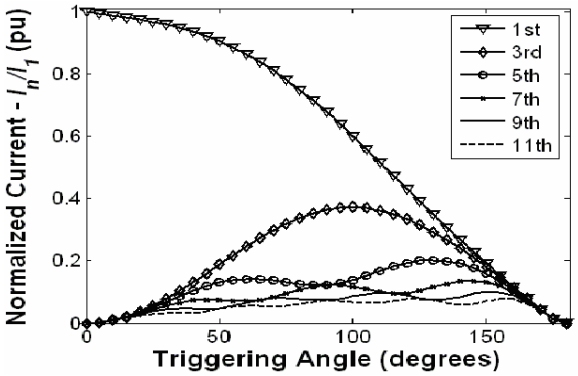

Fig. 3. Six first harmonic components amplitudes.

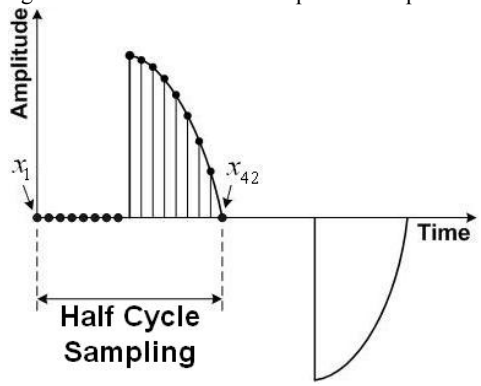

Fig. 4. Sampling process of load current.

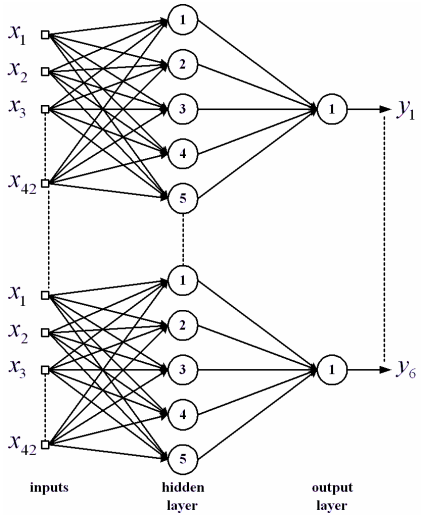

Fig. 5 Feedforward neural network architecture.

The ANN architecture used is the multilayer perceptron (MLP) with supervised training. The neural network basic element is the artificial neuron [18]. The artificial neuron can be modeled by the (8) and (9).

$$v_j(k) = \sum_{i=1}^{m} X_i.w_i + b \tag{8}$$

$$y_j(k) = \varphi_j(v_j(k)) \tag{9}$$

where:

m - Number of input signals of the neuron.
X_i - i-th input signal of the neuron.
w_i - Associated weight with the i-th signal of input.
b - Threshold of the neuron.
$v_j(k)$ - j-th response of the neuron at k instant.
$\varphi_j(.)$ - j-th activation function of the neuron.
$y_j(k)$ - j-th output signal of the neuron.

Each artificial neuron is able to compute the input signal and its respective output. The activation function used to calculate the output signal is typically nonlinear. In this work the ANNs process the analogical data and the adjusting process of the network weights (w_j) associated to the j-th output neuron is done by the error signal calculus $e_j(k)$ (between the desired value $d_j(k)$ and the estimated value $y_j(k)$) in relation to the k-th iteraction or k-th input vector. This error signal is calculated as:

$$e_j(k) = d_j(k) - y_j(k) \tag{10}$$

Adding all squared errors produced by the network output neurons with respect to k-th iteration, we have:

$$E(k) = \frac{1}{2}\sum_{j=1}^{p} e_j^2(k) \tag{11}$$

For an optimized weight configuration, $E(k)$ is minimized regarding the synaptic weight w_{ji}. The weights associated with the output layer of the network are therefore updated using the following relationship:

$$w_{ji}(k+1) = w_{ji}(k) - \eta \frac{\partial E(k)}{\partial w_{ji}(k)} \tag{12}$$

The sinaptic weight w_{ji} is connected to the j-th neuron of the output layer to i-th neuron of previous layer and η is the constant that determines the rate of learning of the backpropagation algorithm. The adjustment of the weights associated to the hidden layers is made of analogous form; the steps for the adjustment are detailed in [18].

The training method is based on the Bayesian regularization, which is used in ANN supervised trainings, using the feedforward algorithm [19]. The approach of Gauss-Newton of the Hessian matrix can be implemented by the structure of the algorithm of Levenberg-Marquadt, reducing the computational effort [19, 20].

The algorithm feedforward, applied in the ANN, use a nonlinear regression. The main objective of this application is to get an algorithm that produces networks with good generalization, restricting the size of the weights matrix, which works as a component of the Bayesian regularization.

Figure 8 to Figure 13 illustrate the ANN results using experimental input signals. The error stopping criterion is of 5.10^{-3}.

The experimental results obtained with the test bench (Figure 6) are illustrated in Figure 7. These results, when compared with simulated data, are limited to the firing angle between 22º and 130º. It occurs due to the constructive limited feature of AC controllers. These controllers are bought in electronic stores and not mounted in laboratory.

RNA is able to converge in all of the estimated outputs, even though the relative errors in some points were relatively high (above 20%, Figure 9 to Figure 13). These errors can occurs because of the low quality of the feeding voltage supplied by the power transformer (Figure 7), in reason of the signal sampling rate of the load current, and due to the noise involved with the instrumentation.

The relative error for each firing angle is acceptable for this application, because the Figure 8 to Figure 13 results demonstrate that the estimated output can be seeking the target output behavior with very close values. In [1] simulation results present error (difference between estimated value and desired value) below 1%.

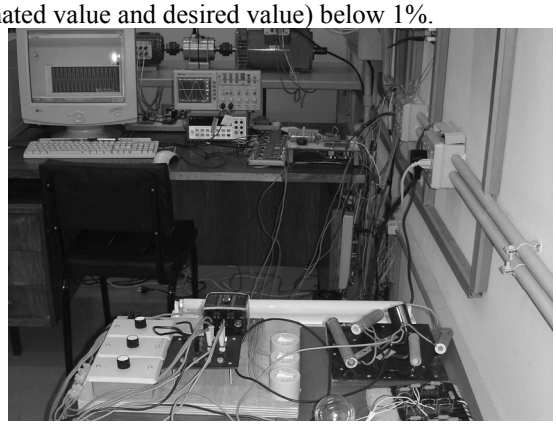

Fig. 6. Test bench of the AC controller circuits.

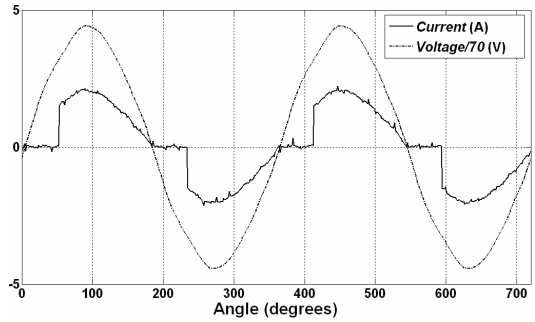

Fig. 7. Experimental load current and voltage source ($\alpha \cong 54º$).

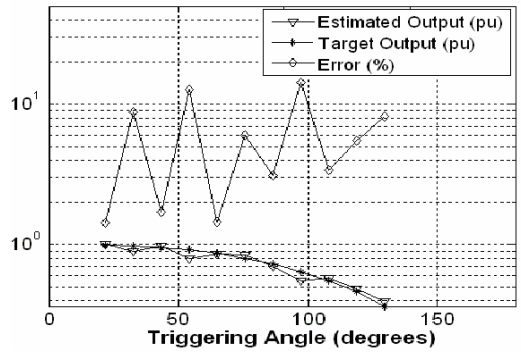

Fig. 8. 1st harmonic content estimation: experimental results.

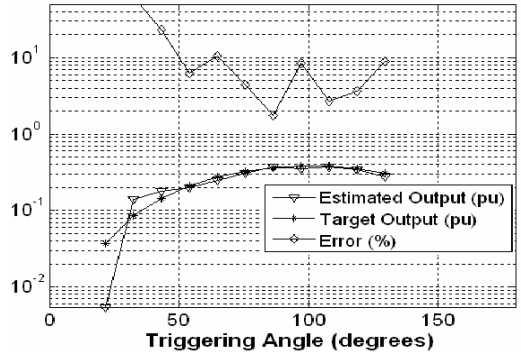

Fig. 9. 3rd harmonic content estimation: experimental results.

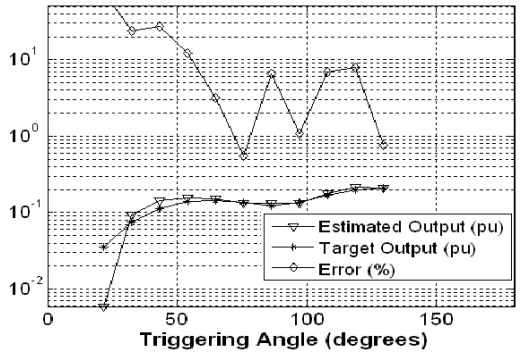

Fig. 10. 5th harmonic content estimation: experimental results.

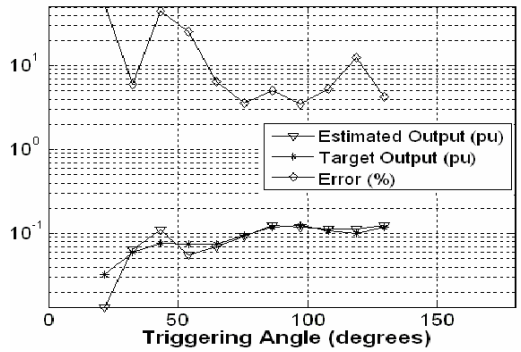

Fig. 11. 7th harmonic content estimation: experimental results.

IV. COMPENSATION HARMONIC

The main simulation results involving the estimated harmonic content, the AC controller and the PAPF are described in this section. It was used the Matlab/Simulink® to simulation of the active power filter [8].

Figure 1 shows the simulated system diagram. In this case, the PAPF injects a harmonic compensation current, as in (13). It is formed by a full bridge PWM inverter in parallel with the AC controller. In this way, the compensation current contain all the harmonics contents which is desirable to be eliminated, but with its phase angles in opposition.

$$i_f(t) = \sum_{n=3}^{11} I_n \sin(n\omega t + \theta_n) \qquad (13)$$

The principle of system operation can be understood in the diagram showed in Figure 14. From the load current harmonic content $\{i_L(t)\}$, the harmonic compensation current $\{i_f(t)\}$ is calculated. In time domain the load current is measured and sampled; afterwards, the amplitudes sampled in half cycle of fundamental are presented to the ANN. With the normalized signal the ANN estimates the six first harmonic components. From this results on the time domain reference current is generated which is used for the system of the PAPF controller. Therefore, the feeding source current provides the fundamental component and the harmonic that are not compensated, i.e.,

$$i_S(t) = i_L(t) - i_f(t) \qquad (14)$$

Figure 15 shows the current source $\{i_S(t)\}$ in the PCC before and after the beginning of the PAPF operation (beginning in the second cycle of fundamental) and a load current $\{i_L(t)\}$.

The proposed method also showed itself effective and robustness when there is a load change. Figure 16 shows the result to a firing angle change, from 90º to 60º in the AC line voltage fourth cycle. In the fifth cycle the PAPF starts the compensation to the angle of 60º. Figure 17 shows the result to the amplitudes change (α = 90º). From the fourth cycle a lamp burns. After one cycle starts the compensation to the system with two lamps.

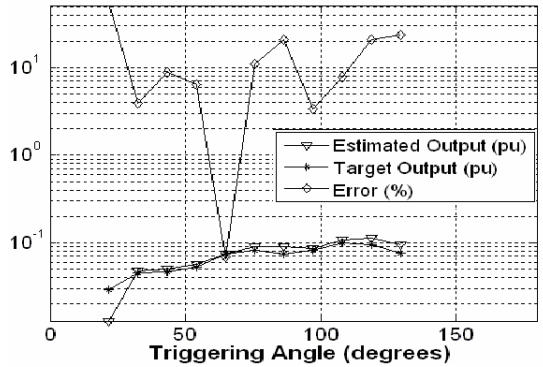

Fig. 12. 9th harmonic content estimation: experimental results.

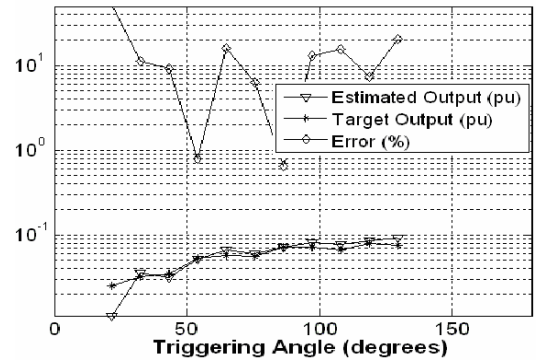

Fig. 13. 11th harmonic content estimation: experimental results.

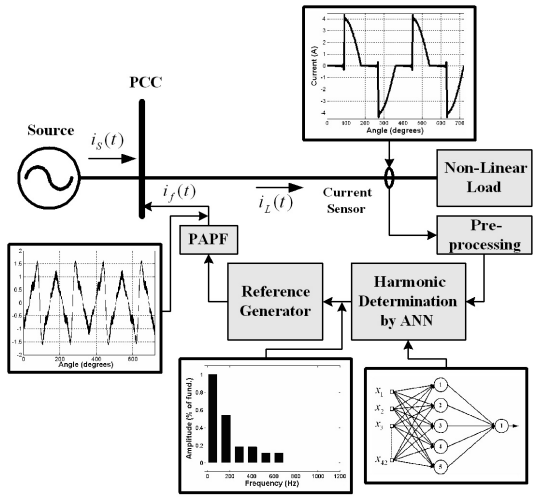

Fig. 14. Simulation diagram of compensation system.

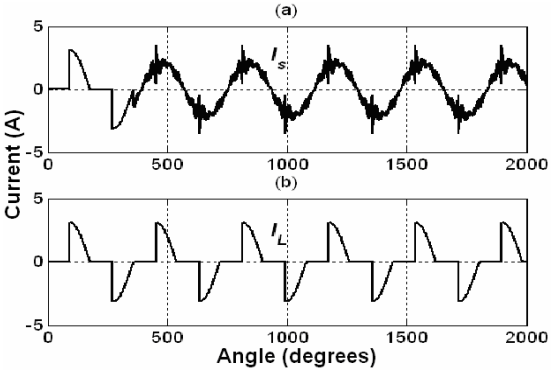

Fig. 15. Compensated current (I_S) (a) and load current (I_L) (b): simulation results.

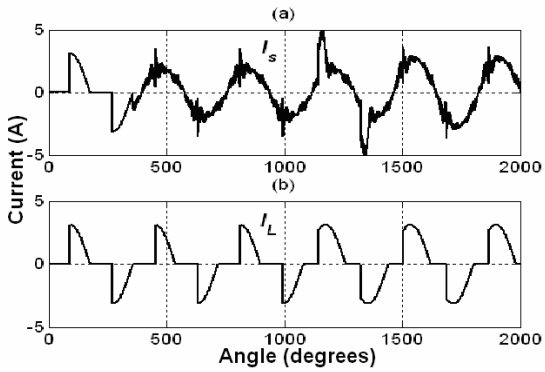

Fig. 16. Compensated current (I_S) (a) and load current (I_L) (b): simulation results.

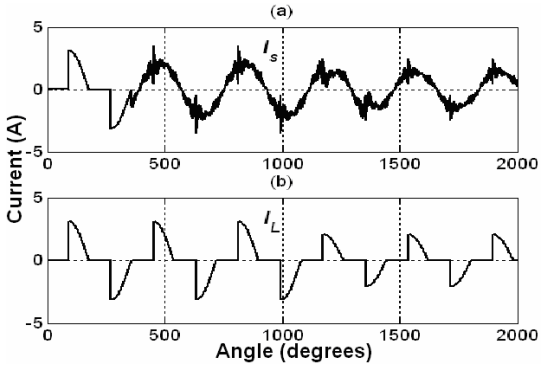

Fig. 17. Compensated current (I_S) (a) and load current (I_L) (b): simulation results.

Figure 18 illustrates the current compensation to a firing angle of 90º. The harmonic power and reactive power are simultaneous compensated by PAPF.

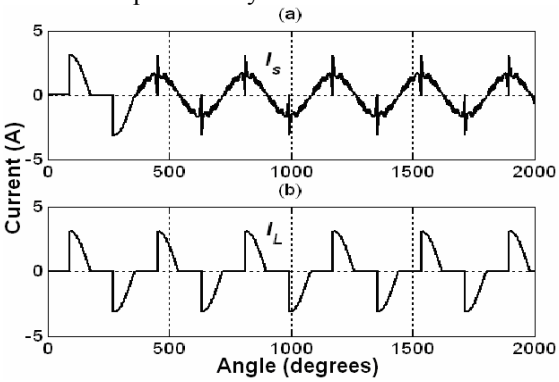

Fig. 18. Compensated current (I_S) (a) and load current (I_L) (b): simulation results.

V. CONCLUSION

An alternative method based on artificial neural network was presented in this work to estimate the harmonic current content of an AC controller. The harmonic content was estimated under harmonics variations with AC controller in steady-state.

The proposed method presented low computational effort and did not demand on sampled signal with certain amount of points for cycle in a certain sampling frequency (witch it is the base of the DFT).

The harmonic content estimation of the AC controller was accomplished set up in a tests bench. The results demonstrate the ANN can estimate the experimental harmonic behavior of the AC controller.

The method based on ANN has been shown able to determine the desirable harmonic content in a half cycle source voltage, and it has an acceptable relative error among the estimated and the desirable value. Therefore, the demands are satisfied in the harmonic determination for a PAPF project.

ACKNOWLEDGEMENT

The authors gratefully acknowledge the support received from CNPq (142128/2005-8 and 142326/2005-4), FAPESP (06/56093-3), and EESC/USP.

REFERENCES

[1] C. F. Nascimento, A. A. Oliveira Junior, A. Goedtel, I. N. Silva, “Compensation current of active power filter generated by artificial neural network approach”, *IEEE IECON’06*, pp. 4392-4397, 2006.

[2] H. Akagi, E. H. Watanabe, M. Aredes, *Instantaneous Power Theory and Applications to Power Conditioning*, John Wiley & Sons, NJ, 2007.

[3] D. A. Torrey, A. Al-Zamel, “Single-phase active power filters for nonlinear multiple loads”, *IEEE Trans. on Power Electron.,* vol. 10, no. 3, pp. 263-271, 1995.

[4] W. M. Grady, M.J. Samotyj, A. H. Noyola, "Survey of active power line conditioning methodologies", *IEEE Trans. on Power Delivery,* vol. 5, no. 3, pp. 1536-1542, 1990.
[5] H. Akagi, "Active harmonic filters", *Proceedings of the IEEE*, vol. 93, no. 12, pp. 2128-2141, 2005.
[6] S. Mariethoz, A. C. Rufer, "Open loop and closed loop spectral frequency active filtering", *IEEE Trans. on Power Electron.*, vol. 17, no. 4, pp. 564-673, 2002.
[7] M. El-Habrouk, M. K. Darwish, "Design and implementation of modified Fourier analysis harmonic current computation technique for power active filters using DSPs", *IEE Proc. Electr. Power Appl.*, vol. 148, no. 1, pp. 21-28, 2001.
[8] A. A. Oliveira Jr, C. F. Nascimento, E. C. C. Cichy, J. R. B. A. Monteiro, M. L. Aguiar, "Introducing the learning of active power filters using the software Matlab-Simulink", *PESC/PEEW 2005. 36th IEEE Power Electronics Specialists Conference*, pp.108-113, 2005.
[9] J. G. Proakis, D. G. Manolakis, *Digital Signal Processing: Principles, Algoritms, and Applications*, 3rd ed., Prentice Hall, NJ, 1996.
[10] C. F. Nascimento, A. A. Oliveira Junior, A. Goedtel, I. N. Silva, "Uma proposta neural para compensação de componentes harmônicos através de um filtro ativo de potência", *VII IEEE Induscon*, QEE-V_4, 2006.
[11] M. Rukonuzzaman, M. Nakaoka, "Single-phase shunt active power filter with harmonic detection", *IEE Proc. Electr. Power Appl.*, vol. 149, no. 5, pp. 343-350, 2002.
[12] L. H. Tey, P. L. So, Y. C. Chu, "Adaptive neural network control of active filters", *Elect. Power Systems Research*, no. 74, pp. 37-56, 2005.
[13] J. R. Vazquez, P. Salmeron, "Active power filter control using neural network technologies", *IEE Proc. Electr. Power Appl.*, vol. 150, no. 2, pp.139-145, 2003.
[14] W. W. L. Keerthipala; L. T. Chong; T. C. Leong, "Artificial neural network model for analysis of power system harmonics", *IEEE Int. Conf. on Neural Networks*, vol. 2, no. 27, pp. 905-910, 1995.
[15] C. Madtharad, S. Premrudeepreechacharn, "Active power filter for three-phase four-wire electric systems using neural networks", *Electric Power Systems Research*, no. 60, pp. 179-192, 2002.
[16] F. Temurtas, R. Gunturkun, N. Yumusak, H. Temurtas, "Harmonic detection using feedforward and recurrent neural networks for active filters", *Electr. Power Systems Research,* no. 72, pp. 33-40, 2004.
[17] R. W. Erickson, *Fundamentals of Power Electronics*, Chapman & Hall, NY, 1997.
[18] S. Haykin, *Neural Networks: Comprehensive Foundation*, Englewood Cliffs, 2nd ed., NJ, 1999.
[19] F. D. Foresee, M. T. Hagan, "Gauss-Newton approximation to Bayesian learning", *Int. Conference on Neural Networks*, vol. 3, pp. 1930-1935, 1997.
[20] M. T. Hagan, M. B. Menhaj, "Training feedforward networks with the Marquardt algorithm", *IEEE Trans. on Neural Networks*, vol. 5, no. 6, pp. 989-993, 1984.